Analysis of a Stochastic Noisy Communication Channel in a Tripartite Synapse with Astrocytes

Giulio Sichili, Laura Galluccio
CNIT Research Unit at University of Catania, Italy
name.surname@unict.it

ABSTRACT

Synaptic plasticity is the ability of synapses to change their strength in response to activity. This process is reputated to underlie learning and memory formation in the brain. Synaptic plasticity can occur through various mechanisms, including long-term potentiation. Astrocyte is one of the actors in regulating synaptic plasticity by releasing signaling molecules which can enhance or inhibit synaptic strength. Indeed the concept of tripartite synapse refers to the functional integration of the presynaptic membrane, postsynaptic membrane, and their interactions with the surrounding astrocytes considered as three synaptic components contributing to lead to synaptic activity. In this paper we investigate on the impact of different types of noise in the context of tripartite synapses. In particular we estimate the effect of axonal noise, as well as calcium influx and astrocyte calcium concentration variation, showing that these noise sources significantly impact on both mutual information and channel opening probability as compared to the case when no noise is assumed.

CCS CONCEPTS

• **Computing Methodologies**; • **Modeling and simulation**;

KEYWORDS

Tripartite Synapse, Astrocytes, Noise, Neuronal Model.

ACM Reference Format:
Giulio Sichili, Laura Galluccio, CNIT Research Unit at University of Catania, Italy. 2023. Analysis of a Stochastic Noisy Communication Channel in a Tripartite Synapse with Astrocytes. In *10th ACM International Conference on Nanoscale Computing and Communication (NANOCOM '23), September 20–22, 2023, Coventry, United Kingdom.*. ACM, New York, NY, USA, 7 pages. https://doi.org/10.1145/3576781.3608720

1 INTRODUCTION

[1]Neuronal communication is a type of molecular communication where the involved cells are neurons responsible for encoding information through the spike rate events and communicating across synapses. Synaptic plasticity is the ability of synapses to change their strength in response to their activity. The relevance of this phenomenon is high, especially when related to learning and memory formation in the brain. Modeling synaptic plasticity is complex due to the numerous physiological mechanisms involved, although some efforts to consider a vesicle release process have appeared [8, 13]. However only few papers address the context of a tripartite synapses [5, 28], where together with the pre and postsynaptic neurons, also *glial cells*, and specifically, *astrocytes*, can support spike generation. In [14] a detailed model of how astrocytes respond to neurotransmitters released from presynaptic neurons by elevating the intracellular calcium levels in astrocytes is presented. Also how, in response to calcium elevations, astrocytes release gliotransmitters including glutamate which may bind to metabotropic glutamate receptors on the astrocyte to activate production of inositol triphosphate (IP3), and consequent increase in calcium concentration inside the astrocyte, is detailed and modeled. Moreover the way in which gliotransmitters can bind to other receptors located on neurons is considered and modeled. However no paper considers additional noise sources in the tripartite synapses process. This instead is the focus of our work. We investigate on the effect of axonal noise as well as calcium influx and astrocyte calcium concentration variation on the tripartite synapses showing that these noise types affect significantly both mutual information and open channel probability as compared to the case where no noise is considered.

The rest of this paper is organized as follows. In Section 2 we provide the background needed for understanding the biological aspects associated to tripartite synapses. In Section 3 we present the proposed model of the tripartite synapse while in Section 4 we detail the noise components of the model. In Section 5 some numerical results are illustrated. Finally, in Section 6 concluding remarks are drawn.

2 FUNDAMENTALS ON ASTROCYTE STRUCTURE

Astrocytes are glial cells exhibiting a typical star shape, which makes them able to envelop a huge number of synapses [1]. Two different classes of astrocyte cells exist in Central Nervous System (CNS): *fibrous astrocytes*, which compose part of the white matter, and *protoplasmic astrocytes*, which are present in the grey matter. The first type of astrocytes are characterized by a limited number of branching, while the second type of cells are more complex and present finer branches. They are involved in several mechanisms inside the CNS, including:

- *Trophic processes*, related to nerve growth factor (NGF) and brain-derived neurotrophic factor (BDNF) [9].

[1]This work was partially supported by the European Union under the Italian National Recovery and Resilience Plan (NRRP) of NextGenerationEU, partnership on "Telecommunications of the Future" (PE0000001 - program "RESTART").

NANOCOM '23, September 20–22, 2023, Coventry, United Kingdom

ACM ISBN 979-8-4007-0034-7/23/09.
https://doi.org/10.1145/3576781.3608720

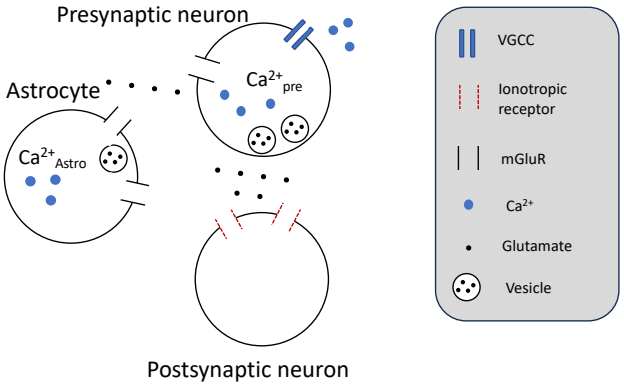

Figure 1: Schematic of a Tripartite Synapse.

- *Regulating homeostasis* [7] associated to buffering extracellular K+, controlling the neurotransmitter release, establishing the blood-brain barrier (BBB), and controlling the immunological response in the brain.
- *Synaptic regulation*, related to the fact that astrocytes play both a role in inhibitory and excitatory synapses [2].
- *Synaptic plasticity*, because astrocytes impact in particular on Long-Term Potentiation (LTP) in the tripartite synapse which consists of a persistent strengthening of the synapse based on current patterns of activity. These patterns result in a long-lasting increase in signal transmission between two neurons. The importance of LTP is also related to the fact that this is the primary, although not the only, cellular mechanisms driving learning and memory, which is indeed typically assumed to be conveyed via alteration of synaptic strength [3, 4].

The majority of the synapses in the CNS are classified as chemical, meaning that the information is conveyed by molecules (usually proteins), and in particular *neurotransmitters*, e.g. adrenaline, glutamate, exchanged between neurons, and *gliotransmitters*, i.e. signaling molecules emitted by glial cells. For worth of illustration, although not all synapses are identical, let us consider an excitatory synapse (i.e. a synapse releasing an excitatory neurotransmitter that moves the post-synaptic neuron membrane potential toward its threshold for firing) in the hippocampal region. The axon hillock is the site in the cell soma where action potentials, once generated from the synaptic inputs, are transmitted to the axon. During their propagation along the axon, possible noisy effects due to the unmyelinated axon can be met as discussed in the following. After propagation along the axon, the action potential comes to the *synaptic boutons* which are small swellings found at the terminal ends of axons and representing the sites where synapses with other neurons are located, and where neurotransmitters are stored. Here the signal triggers voltage-gated calcium channels (VGCCs) Ca^{2+} injection in the cytosol, that ultimately cause evoked vesicle release via SNARE protein complex binding with calcium ions, making possible exocytosis of glutamate vesicles in the synaptic

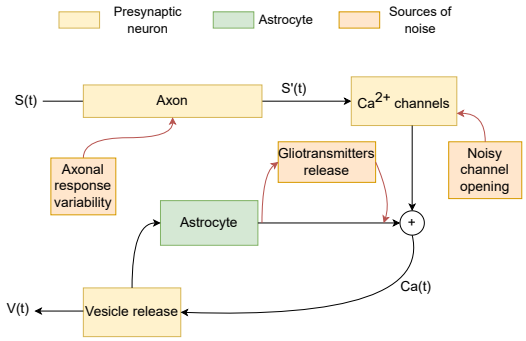

Figure 2: Functional scheme of the tripartite synapse including noise sources.

cleft. At this stage, part of glutamate binds to ionotropic receptors AMPAR (α-amino-3-hydroxy-5-methyl-4-isoxazolepropionic acid receptor) and NMDAR (N-methyl-D-aspartate receptor) on the postsynaptic neuron, conveying information via excitatory postsynaptic potentials; a fraction of the released glutamate instead binds to metabotropic receptors on the astrocyte. Metabotropic glutamate receptors (mGluRs) are involved in inositol triphosphate (IP3) production, a molecule whose role is fundamental in the tripartite synapse: binding to IP3 receptors in the astrocyte Endoplasmic Reticulum (ER), a positive Ca^{2+} current is elicited, and the uprising of calcium concentration inside astrocyte triggers the release of gliotransmitters which ultimately cause the production of IP3 and the release of calcium, in the presynaptic neuron, leading to a positive feedback mechanism. A biological schematic of a tripartite synapse is shown in Fig. 1 while a functional representation of the involved actors and their interactions are sketched in Fig. 2.

3 MODEL DESCRIPTION

In modeling the tripartite synapse as a communication channel let us consider the process of an action potential spike generated in the axon hillock and arriving at the axonal terminal at time t, i.e. $S(t)$ as input, and let us focus on the vesicle release process at time t occurring as a consequence of the spiking event. We denote this output process as $V(t)$. As shown in Fig. 2, the following phases can be identified in the process of conversion of the input signal into the output one:

(1) *Vesicle release* in the presynaptic terminal;
(2) *Calcium concentration variation* in the presynaptic terminal;
(3) *Astrocytic response.*

In the following subsections, we analyze the characteristics of the involved processes.

3.1 Spike generation

We consider the action potential (AP) emission process $S(t)$ as an inhomogeneous Poisson process characterized through a parameter $\lambda(t)$ [18] which is the instantaneous spike rate (spikes/s). Also we assume time is slotted in small intervals of duration Δt chosen so as to be much smaller than the so called *absolute refractory period* [14] which represents, for a neuron, the time of inactivation of sodium channels after a firing and is the time interval when, after

a previous spiking event, due to inactivation, a new spike cannot occur.

With this choice of Δt, it is guaranteed that at most a single firing event can happen in each time interval.

The spike probability in a small Δt interval can be thus calculated as [14]:

$$P\{S(t, t+\Delta t) = 1\} = 1 - exp(-\lambda(t)\Delta t). \quad (1)$$

In our model we consider that time is slotted; so in the rest of the paper we refer to $P\{S(t+(n-1)\Delta t, t+n\Delta t) = 1\}$ simply as $P\{S[n] = 1\}$, where n is the $n-th$ time interval of duration Δt.

3.2 Vesicle release in the presynaptic terminal

Synaptic vesicles are structures in neurons apt to store different neurotransmitters which are released at synapses. The release is controlled through voltage-dependent calcium channels. The cell constantly produces new vesicles because they are necessary for transmitting nerve pulses between neurons.

Vesicular release mechanisms can be classified in two categories: [14]:

- *Evoked* vesicular release occurring during an AP.
- *Spontaneous* vesicular release when no AP is received.

Both processes can be modeled as inhomogeneous Poisson processes [18], with rates of $\lambda_v(t)$ and $\lambda_0(t)$, respectively.

The evoked vesicle release depends on the probability of the membrane to be depolarized (i.e. an AP being currently received). In this case, at the axon terminal, due to the opening of voltage dependent calcium channels (VDCCs), an incoming flux of calcium ions is received, which diffuse in the terminal at the sensors close to the vesicles. When the density of calcium ions at sensors is sufficiently large, the process of fusion of vesicles with the membrane starts. Indeed, some vesicles that can be immediately released in response to stimulation (forming the so called rapidly releasable pool (RRP)), are docked to the cell membrane. Since this pool of vesicles, immediately usable, is limited and quickly depleted, a backup set denoted as unavailable pool (UP) larger than the quickly releasable pool, but taking longer to mobilize is available. This UP is needed to implement a release and replenishment model to keep the vesicle release mechanism always active.

When evoked vesicle release is activated, four sites for Ca^{2+} binding are available [22], each in general characterized through different rates for closing and opening.

Accordingly, by assuming that opening and closing of each of the four binding sites can be modeled as an independent process, the probability of activation for the release site as a consequence of the AP, $O_{ch}(t)$ can be written as the product of the different opening probabilities $O_j(t)$, j=0,1,2,3, which dynamics can be described as [31]:

$$\frac{dO_j(t)}{dt} = k_j^+ Ca_{pre}(t) - \frac{O_j(t)}{\tau_j}, \quad (2)$$

where values of the constants k_j^+ and k_j^- for the different binding sites are detailed in [31], $Ca_{pre}(t)$ is the presynaptic calcium concentration and will be detailed and discussed in the following and τ_j represents the reciprocal of the quantity $[k_j^+ Ca_{pre}(t) + k_j^-]$.

For the splitting property of Poisson processes [14], evoked vesicle release rate is given as

$$\lambda_v(t) = O_{ch}(t)\lambda(t) \quad (3)$$

where $O_{ch}(t)$ is defined as $O_{ch}(t) = \Pi_{j=0}^{3} O_j(t)$.

The probability to have, in case of evoked potential, a vesicular release for hippocampal neurons, can be thus written as

$$P\{V[n] = 1|S[n] = 1\} = \begin{cases} 1 - e^{-N\beta(\Delta t)} & \Delta t \le \tau_{AP} \\ 1 - e^{-N\beta(\tau_{AP})} & \Delta t > \tau_{AP} \end{cases} \quad (4)$$

where τ_{AP} is the action potential spike duration, N is the number of available vesicles and $\beta(\Delta t)$ is the fusion rate at each vesicle which represents the integral of the evoked vesicle release in a given time slot Δt. More specifically, from eq. (3) we have that

$$\beta(\Delta t) = \int_{\tau_0}^{\tau_o + \Delta t} O_{ch}(t) \cdot \lambda(t) dt \quad (5)$$

The spontaneous vesicle release process, instead, does not depend on the arrival of an AP and can be modeled as [23]

$$\lambda_0(t) = \delta_3 \left(1 + exp\left(\frac{\delta_1 - Ca_{pre}(t)}{\delta_2}\right)\right)^{-1}, \quad (6)$$

where δ_1, δ_2 and δ_3 values are taken from [14], where only one active zone [22] is considered.
Accordingly in case of spontaneous release, the probability that a synapse with N available vesicles, leads to a release in a time slot of duration Δt can be written as

$$P\{V[n] = 1|S[n] = 0\} = 1 - e^{-N\lambda_0(t)\Delta t} \quad (7)$$

While the mechanism of the neurotransmitter release in the synaptic cleft associated to vesicle exocytosis is well known [17], the exact physiological and functional distinction between these two phenomena (evoked and spontaneous vesicle release) is still a matter of debate [11]. A common hypothesis is that the same vesicle pool is involved in the two processes.

By considering the two above mentioned vesicle release mechanisms, the overall probability of a vesicle release in a specific Δt time interval, can be written as:

$$P_v(\Delta t) = \begin{cases} O_{ch}(\Delta t); & \text{AP active} \\ 1 - exp(-N\lambda_0(t)\Delta t) & \text{otherwise.} \end{cases} \quad (8)$$

and

$$O_{ch}(\Delta t) = \frac{1}{\Delta t} \int_t^{t+\Delta t} O_{ch}(\tau) d\tau \quad (9)$$

upon considering that $[t, t+\Delta t] \subseteq [t^{(f)}, t^{(f)} + \tau_{AP}]$ where $t^{(f)}$ is the firing time.

3.3 Calcium concentration variation

Calcium concentration variation inside the presynaptic terminal can be modeled by considering two different mechanisms, which happen at different timescales:

- *Fast* calcium dynamics impacting on calcium concentration, described via the term $Ca_{fast}(t)$, which considers calcium entering via VGCCs activated because of AP. This fast mechanism decays in about 100ms after the AP event.

- *Slow* calcium dynamics impacting on calcium concentration, described via the term $Ca_{slow}(t)$, which is caused by the mGluRs-IP3 release pathway via ER, and modulated by astrocytic feedback. The increase of calcium concentration due to the glutamate released by the astrocyte and bound to the receptors at the presynaptic terminal, boostes intracellular calcium concentration $Ca_{slow}(t)$ thus supporting spontaneous vesicle release. The effect of this phenomena is to lead to a boost in the synaptic activity on much larger time scales (approximately 1 minute).

So it follows that:

$$Ca_{pre}(t) = Ca_{fast}(t) + Ca_{slow}(t) \tag{10}$$

The calcium concentration variation due to slow dynamics can be described by considering a leakage parameter γ_{slow} and a positive linear relationship with the parameter representing the concentration of calcium in astrocytes, $Ca_{Astro}(t)$[2]. More specifically, it is:

$$\frac{dCa_{slow}(t)}{dt} = -\gamma_{slow} Ca_{slow}(t) + \alpha \cdot Ca_{Astro}(t) \cdot \cdot H[Ca_{Astro}(t) - Ca_{thresh}], \tag{11}$$

where α is a feedback strength parameter described in [22] and $H[c - c_0]$ is the Heaviside step function centered in c_0.

3.4 Astrocyte dynamics

Astrocytes play a relevant role in LTP. In particular, the glutamate issued by neuronal cells is bound to metabotrobic glutamate receptors (mGluRs) which are available at astrocytes. As a consequence, IP3, which is a second messenger can be generated and binds to the appropriate IP3 receptors located on top of the ER. As an effect of this, calcium is released inside the astrocyte which on its turn leads to glutamate release. This glutamate binds to mGluRs receptors [25] at the presynaptic terminal, thus causing potentiation in the synaptic transmission mechanism with a consequent release of calcium at the presynaptic terminal. To well characterize this phenomen, a characterization of the variation of IP3 concentration p in time is possible as

$$\frac{dp}{dt} = -\frac{1}{\tau}(p - p_0) + v_p \frac{Ca_{Astro}(t) + 0.2k_p}{k_p + Ca_{Astro}(t)} + v \frac{g^n}{k_g^n + g^n} \Pi\left(\frac{t - (t^{(f)} + 0.5 \cdot T_{glu})}{T_{glu}}\right) \tag{12}$$

Production and degradation constants τ, v_p, p_0, k_p, g^n, k_g^n are detailed in [22] while $\Pi\left(\frac{t-(t^{(f)}+0.5\cdot T_{glu})}{T_{glu}}\right)$ is a rectangular function of duration equal to glutamate persistance in the synaptic cleft, i.e. T_{glu}. IP3 concentration impacts on one of the 3 ionic fluxes that contribute to cytosolic Ca^{2+} evolution inside the astrocyte: in particular IP3 concentration impacts on IP3 receptor channels flux, denoted as $J_{channel}$. Specifically, the inhibition of calcium due to the increase in concentration of cytosolic calcium can be represented by the well known Li-Renzel model [16, 29] through the inhibition parameter q. Thus, the variation in the concentration of calcium at astrocytes can be written as [22]

$$\frac{dCa_{Astro}(t)}{dt} = -J_{channel}(q) - J_{pump} - J_{leak}. \tag{13}$$

Parameters J_{pump} and J_{leak} represent the Sarco Endoplasmic Reticulum ATPase (SERCA) active transporter inducted flux, and the leakage component, respectively. Exact computation of J_{pump} and J_{leak} is reported in [30].

We focus on $J_{channel}$ as this flux is actively modulated by IP3 concentration [22]. In particular it can be shown that[3]:

$$\begin{cases} J_{channel}(q) = c_1 v_1 m_\infty^3 n_\infty^3 q^3 (Ca_{Astro} - Ca_{ER}) \\ \frac{dq}{dt} = \alpha_q(1 - q) - \beta_q q + \xi_q(t) \\ \alpha_q = a_2 d_2 \frac{p+d_1}{p+d_3};\ \beta_q = a_2 Ca_{Astro};\ m_\infty = \frac{p}{p+d_1} \end{cases} \tag{14}$$

Parameter q is the gating variable of IP_3R [30] and is responsible for delay in activation of astrocytic feedback, coherently with the notion of LTP. This mathematical description [16] predicts oscillation for astrocytic calcium concentration [22]. Note that we have included a stochastic term $\xi_q(t)$ in eq. (14) for describing the variation in the inhibition parameter q. This is derived from the Langevin equation, and eqs. (12)-(14) globally report a stochastic version of the Li-Rinzel model.

4 NOISE COMPONENTS IN THE MODEL

In this section we detail possible noise sources impacting on the tripartite synapse mechanism. More specifically, differently from what is described in the literature, we incorporate in our model this investigation so as to estimate the impact of noise on the astrocyte action at the synapse. In the following subsections we will discuss the effect of axonal noise, variability in Ca^{2+} influx as well as a noise component generated by astrocytes themselves.

4.1 Axonal noise

While being often considered transparent to signal transmission, axon has been proved to have a significant effect in neuronal communication [24], and being able both to either interfere and block AP propagation and/or to modify waveforms [6, 10, 19], especially in case of unmyelinated axons [20]. A study in [24] has proposed a direct correlation between axonal diameter and variability in action potential amplitude and duration. The impact of channel opening fluctuations on AP waveform increases for smaller axons, since variations of few channels can lead to oscillations which are numerically comparable to the absolute value of the membrane voltage.

Here we consider the coefficient of variation (CV) of waveform fluctuations defined as the ratio of the standard deviation over the mean for the metric which identifies variability in waveforms as proposed in [24]. We include this stochastic behavior in our model, assuming to refer to an unmyelinated axon with diameter of 0.2μm as common in cerebellar parallel fibres. We propose a phenomenological model which describes the mutation between the spike train at the proximal site $S(t)$, and the respective modified spike train $S'(t)$ measured at the distal site (see Fig. 2). Accordingly, we derive the axonal impulse response at discrete time instants, $a[n]$ given that we are assuming that $a(t)$ remains constant for

[2]Note that calcium is released from presynaptic stores only when Ca_{Astro} concentration is larger than Ca_{thresh} which is an appropriate threshold parameter of activation.

[3]All parameters and coefficients in the model are described in [22].

a time interval t_{ax} larger than τ_{AP}. The expression of the axonal impulse response can be stochastically derived according to the parameters of CV found in [6, 24, 26]. Three parameters are needed to characterize the output spike train:

(1) Variation in Inter-spike intervals (jitter) [6, 15];
(2) Modulation in amplitude, where amplitude of the AP is defined as the maximum membrane voltage, typically in the order of mV [24, 26];
(3) Variability in AP duration which is in the order of ms [24].

The first two parameters mentioned above can be employed for the characterization of the axonal impulse response as:

$$a(t) = \phi(\xi_{amp}, \xi_{delay}) \tag{15}$$

with ξ_{amp} and ξ_{delay} Gaussian variables with standard deviation $\sigma_i = CV_i \times \mu_i$, with $i \in \{amp, delay\}$ and mean value μ_i. Concerning the variability in the AP duration. It can be modeled as a random variable with Gaussian probability distribution function centered in τ_{AP} and characterized by a standard deviation derived from [24].

The resulting action potential emission process $S'(t)$ can be thus obtained through convolution between the original $S(t)$ and $a(t)$. Moving to the discrete domain, it thus follows that

$$S'[n] = S[n] * a[n] \tag{16}$$

where $*$ denotes the convolutional operator.

4.2 Variability in Ca^{2+} influx from channels

As studied in [21], the noise component which plays the most relevant role on calcium influx inside the cell and on the vesicle release process, is associated to the stochastic openings of VGCCs, as compared to diffusion and receptor kinetics. Indeed in [27], the VGCCs-mediated Ca^{2+} influx rather than Calcium binding to sensors, Calbindin buffers or PMCA pumps are stochastically modeled. According to this previous formulation, the VGCC-mediated calcium influx probability distribution can be included as a noisy contribution. We derived the average waveform for Ca_{fast} from modified version of the typical construction-deconstruction formalism [12] from [30], where we imposed a first order decaying relationship for simplicity:

$$\frac{dCa_{fast}(t)}{dt} = \frac{I_{ch}(t)A_{btn}}{z_{Ca}FV_{btn}} - \gamma_{fast}Ca_{fast}(t) \tag{17}$$

with

$$\begin{aligned} I_{ch}(t) &= I_{ch,avg}(t) + \xi_{ch} \\ I_{ch,avg}(t) &= n_{ch}O_{ch}(t)g_{Ca}(V_{Ca} - V_{pre}(t)). \end{aligned} \tag{18}$$

In the above equations, $I_{ch}(t)$ is the Ca^{2+} current, A_{btn} is the area of the synaptic bouton, z_{Ca} is the Ca^{2+} ion valence, F is the Faraday constant, V_{btn} is the volume of the synaptic bouton and γ_{fast} is a calcium leakage parameter. Also parameters in eq. (18) which is derived considering a single protein level formulation are the presynaptic membrane potential $V_{pre}(t)$, the reversal potential of the Ca^{2+} ion V_{Ca} which can be obtained from the Nernst equation [12], the calcium conductance g_{Ca}, and the channel density n_{ch}.

Then, in order to add a stochastic component ξ_{ch} to the Ca^{2+} current, in eq. (18) we resort to a model similar to the one presented in [27]. More specifically, we use a logistic distribution for positive noise values, and a normal distribution for negative ones. As a consequence, in eq. (18), ξ_{ch} is a random current contribution whose pdf is defined as:

$$\begin{aligned} f_{\xi_{ch}}(x|o,s) &= \begin{cases} f_N(x|o,\sigma_n(t)) & x \le 0 \\ f_L(x|o,s(t)) & x > 0 \end{cases} \\ s(t) &= \sqrt{3} \cdot \sigma_p(t)/\pi \\ \sigma_n(t) &= a_n\sqrt{0.5 \cdot I_{ch,avg}(t)/(e \cdot n_{ch})}; \\ \sigma_p(t) &= a_p\sqrt{0.5 \cdot I_{ch,avg}(t)/(e \cdot n_{ch})}, \end{aligned} \tag{19}$$

In the above equation, a_n and a_p are parameters derived from microphysiological simulations where typically $a_n = 250$ and $a_p = 350$.

Then we computed the resulting Ca_{fast} waveform from (17) and chose a scale parameter to reproduce an average concentration of 300μM during the 2ms following AP initiation [23].

4.3 Noise generated by the astrocyte

In Section 3.3 we assumed a linear relationship between the stored presynaptic calcium concentration and the astrocytic calcium concentration in eq.((11)), meaning that each time $Ca_{Astro}(t)$ is larger than Ca_{thresh}, presynaptic calcium concentration increases and similarly the corresponding release probability. A more realistic hypotesis would be to take into account that, similarly to what happens in the synaptic bouton, as explained in Section 3.2, neurotransmitters (specifically gliotransmitters) are diffused in the synaptic cleft through a mechanism of vesicle exocitosis in the astrocyte as well. We specifically define an ideal astrocyte vesicular release rate as $\lambda_a(t)$ which represents the rate at which the astrocyte would ideally release a vesicle. Then, we consider as the effective release rate, the product of the ideal rate and the instantaneous calcium concentration in the astrocyte, i.e.:

$$P_{v,a}(t) = 1 - exp\left(-\lambda_a(t)Ca_{Astro}(t)\right). \tag{20}$$

In this way, due to the instability in the astrocytic calcium concentration, effective rate results lower than the ideal rate.
Once a vesicle is released by the astrocyte, presynaptic calcium concentration starts increasing as in eq.(11), but only for a period of time that we assume equal to glutamate reabsorbtion time in the synaptic cleft, to simulate reuptake. More specifically, :

$$\begin{aligned} \frac{dCa_{slow}(t)}{dt} &= -\gamma_{slow}Ca_{slow}(t) + \alpha Ca_{Astro}(t)\cdot \\ H[Ca_{Astro}(t) - Ca_{thresh}]&\Pi\left(\frac{t - (t^{(f)} + 0.5 \cdot T_{glu})}{T_{glu}}\right). \end{aligned} \tag{21}$$

5 NUMERICAL ANALYSIS

In this section we report some preliminary results on the stochastic model presented in the previous sections. More specifically we first illustrate the metrics considered in our investigation, and then we illustrate numerical results.

5.1 Metrics

We focus our observation on performance metrics that well describe the quality of the neuronal communication channel. To this aim we consider a parameter representing the amount of information

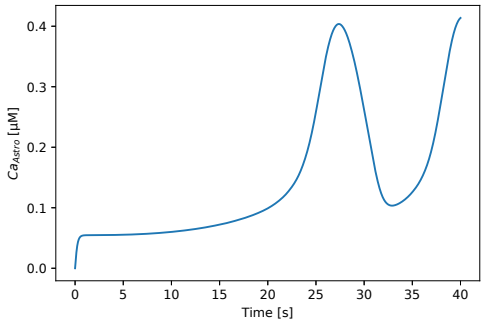

Figure 3: Concentration of Calcium at the astrocyte (in μM) vs. time from eq. (13).

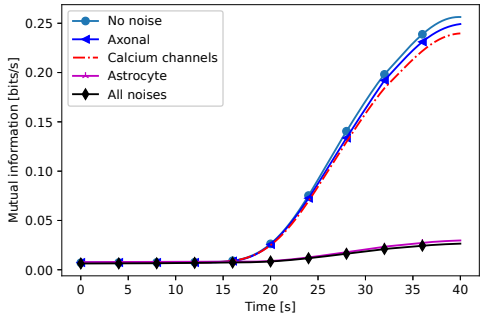

Figure 4: Mutual information vs. time for the tripartite synaptic model $\lambda = 20Hz$.

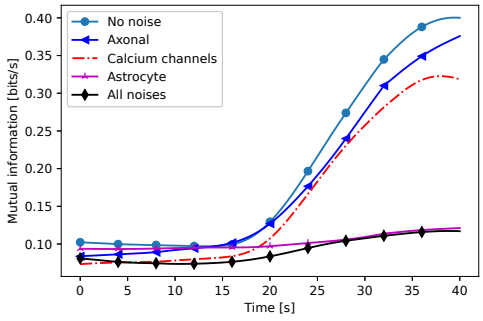

Figure 5: Mutual information vs. time for the tripartite synaptic model $\lambda = 100Hz$.

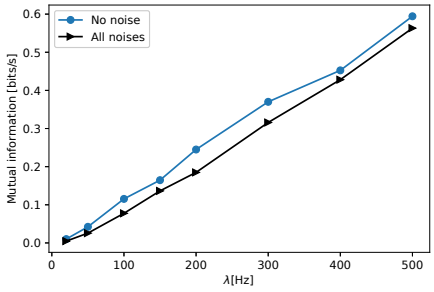

Figure 6: Average mutual information obtained for 2s of stimulation in the early LTP zone vs. λ (Results averaged over 20 simulations).

which can be conveyed by exploiting the spike train process in combination with the vesicle release process, i.e. the mutual information. The mutual information can be traditionally expressed as

$$I(S[n];V[n]) = H(V[n]) - H(V[n]\,|\,S[n]), \tag{22}$$

where $H(V[n])$ is the marginal entropy of $V[n]$ and $H(V[n]\,|\,S[n])$ is the conditional entropy. Since both $S[n]$ and $V[n]$ can only take values 0 and 1, the entropy can thus be written as

$$H(X[n]) = -P(X[n]=1)log_2P(X[n]=1)- \\ -P(X[n]=0)log_2P(X[n]=0).$$

where in general $X[n]$ can be either identified with $V[n]$ or $S[n]$.

Then we also present results on the average mutual information which can be computed as $Av_I = \sum_{i=1}^{n} \frac{I(S[i];V[i])}{n}$.

Another parameter of interest is the opening channel probability which can be derived as in eq. (2). This parameter gives information about probability of a vesicular release, given that the membrane is depolarized, which gives an estimation of the efficacy of the synaptic output.

5.2 Results

In this subsection we illustrate some preliminary results obtained through simulations. All plots consider that the AP emission process is characterized through $\lambda \in \{20, 100, 200\}$ Hz and N_{max} is the maximum number of releaseble vesicles is fixed and equal to 10 (few releaseable vesicles), or 27 (many releaseable vesicles). In our simulations [30], we assume a refractory period $\tau_{ref,v}$ of 6.34ms for vesicle release for both neurons and astrocytes. Also we investigate on the time evolution of vesicle release probability with and without considering the 3 types of noise.

In Figs. 4 and 5 we report the mutual information for the tripartite synaptic model with and without considering the noise effect, for two different values of λ. Observe that all plots show an abrupt rise after about 20s from the beginning of the simulation, showing the effect of astrocyte feedback as explained in Section 3 and as also visible in Fig. 3. It turns out that after a period of stimulation with a constant spike rate $\lambda = 100Hz$, astrocytic calcium reaches the threshold of 196.4nM only when the IP3 gating variable q becomes larger than about 0.7. Indeed in our simulations this happens after approximately 20-25s. Hence, we used this condition to simulate the neuron in conditions of LTP, so initializing $q(0) = 0.7$ also in the other experiments. Note that in both plots, the impact of noise is relevant meaning that a remarkable variation in the mutual information is obtained upon increasing the noise contribution. Specifically, the astrocytic noise is the one that results more critical in the system because it modifies the effective release rate taking into account the instantaneous calcium concentration in the astrocyte which, as evident in Fig. 3, significantly decreases after approximately 28s.

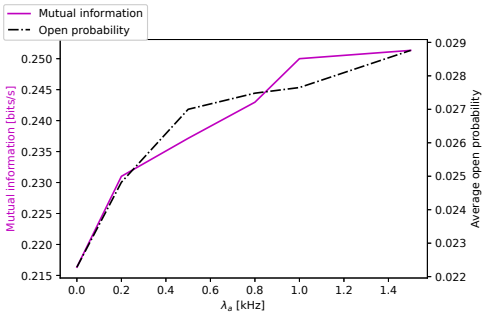

Figure 7: Average mutual information and average open channel probability vs. λ_a obtained for 5s of stimulation in the early LTP zone (λ=200 Hz).

In Fig. 6 we show the average mutual information vs. λ. Note that an approximately linear trend is exhibited. Noisy curves follow a similar behavior laying beneath the noiseless curve. This suggests again a slight reduction in channel capacity in presence of the considered stochastic components, regardless of the frequency of the input provided. However note that this reduction is however quite limited and constant and remains in the order of 0.02 bits/(s Hz). By having identified the criticality resulting from the consideration of the astrocytic noise caused by the variation in the astrocyte vesicular release rate, in Fig. 7 we show the mutual information and the average open channel probability as a function of the astrocytic vesicle release rate λ_a. Note that the mutual information increases as a function of the λ_a parameter which highlights the relevant effect played by the astrocytic vesicle release mechanism. Also, concerning the average open probability, an almost logarithmic trend is exhibited as function of λ_a, again showing that for relatively small values of λ_a the curve has a rise, while higher values of λ_a would not help much more in obtaining more vesicle release in the presynaptic vesicle. The limit imposed by vesicle release refractory period must also be considered as likely source of limitation in the effective release rate.

6 CONCLUSIONS

Recent literature has shown the importance of considering the action of astrocytes in neuro-spike transmission. These play a key role in learning processes as related to synaptic plasticity. In this paper we have provided a preliminary stochastic noise modeling of the tripartite synapse. We have focused on the contribution of axonal noise, variability in Ca^{2+} influx and noise generated by the astrocyte itself as a consequence of a stochastic variation in the calcium concentration. We have estimated the different contributions of these noise sources in terms of mutual information and open channel probability, showing that these effects cannot be neglected and need to be accounted in realistic investigations on LTP.

REFERENCES

[1] N.J. Allen. 2014. Synaptic Plasticity: Astrocytes Wrap It Up. *Current Biology* 24, 15 (2014), R697–R699. https://doi.org/10.1016/j.cub.2014.06.030

[2] J. V. Andersen, A. Schousboe, and P. Wellendorph. 2023. Astrocytes regulate inhibitory neurotransmission through GABA uptake, metabolism, and recycling. *Essays Biochem* 67, 1 (Mar 2023), 77–91.

[3] S.F. Cooke. 2006. Plasticity in the human central nervous system. *Brain* 8, 3 (2006). https://doi.org/10.1038/361031a0.PMID8421494

[4] S. F. Cooke. 2006. A synaptic model of memory: long-term potentiation in the hippocampus. *Nature* (2006).

[5] P. A. Floor F. Mesiti and I. Balasingham. 2015. Astrocyte to neuron communication channels with applications. *IEEE Trans. Mol. Biol. Multi-Scale Commun.* 1, 2 (2015).

[6] A. A. Faisal and S. B. Laughlin. 2007. Stochastic simulations on the reliability of action potential propagation in thin axons. *PLoS Comput Biol* 3, 5 (May 2007), e79.

[7] J. R. Gee and J. N. Keller. 2005. Astrocytes: regulation of brain homeostasis via apolipoprotein E. *Int J Biochem Cell Biol* 37, 6 (Jun 2005), 1145–1150.

[8] T. Khan H. Ramezani and O. B. Akan. 2018. Information theoretical analysis of synaptic communication for nanonetworks. *IEEE Infocom* (2018).

[9] L. M. Holt, R. D. Hernandez, N. L. Pacheco, B. Torres Ceja, M. Hossain, and M. L. Olsen. 2019. Astrocyte morphogenesis is dependent on BDNF signaling via astrocytic TrkB.T1. *Elife* 8 (Aug 2019).

[10] J. R. Huguenard. 2000. Reliability of axonal propagation: the spike doesn't stop here. *Proc Natl Acad Sci U S A* 97, 17 (Aug 2000), 9349–9350.

[11] E. T. Kavalali. 2015. The mechanisms and functions of spontaneous neurotransmitter release. *Nat Rev Neurosci* 16, 1 (Jan 2015), 5–16.

[12] J. Keener and J. Sneyd. 1998. *Mathematical Physiology.* Springer-Verlag, Berlin, Heidelberg.

[13] T. Khan and O. B. Akan. 2019. Sum rate analysis of multiple-access neuro spike communication channel with dynamic spiking threshold. *Nano Commun. Netw.* 19 (2019).

[14] T. Khan and O. B. Akan. 2022. Communication Theoretical Modeling and Analysis of Tripartite Synapses With Astrocytes in Synaptic Molecular Communication. *IEEE Trans. on Mol., Biol. and Multi-Scale Comm.* 8, 3 (2022).

[15] L. Kostal and P. Marsalek. 2009. Neuronal jitter: can we measure the spike timing dispersion differently? *BMC Neuroscience* 10 (2009), 1.

[16] Y. X. Li and J. Rinzel. 1994. Equations for InsP3 receptor-mediated [Ca2+]i oscillations derived from a detailed kinetic model: a Hodgkin-Huxley like formalism. *J Theor Biol* 166, 4 (Feb 1994), 461–473.

[17] R. C. Lin and R. H. Scheller. 2000. Mechanisms of synaptic vesicle exocytosis. *Annu Rev Cell Dev Biol* 16 (2000), 19–49.

[18] D. Malak and O. B. Akan. 2013. A Communication Theoretical Analysis of Synaptic Multiple-Access Channel in Hippocampal-Cortical Neurons. *IEEE Trans. on Comm.* 61, 6 (2013).

[19] J. P. Meeks, X. Jiang, and S. Mennerick. 2005. Action potential fidelity during normal and epileptiform activity in paired soma-axon recordings from rat hippocampus. *J Physiol* 566, Pt 2 (Jul 2005), 425–441.

[20] Grider M.H., R. Jessu, and R. Kabir. 2023. Physiology, Action Potential. *StatPearls [Internet] Treasure Island (FL): StatPearls Publishing* (2023).

[21] C. Modchang, S. Nadkarni, T. M. Bartol, W. Triampo, T. J Sejnowski, H. Levine, and W.-J. Rappel. 2010. A comparison of deterministic and stochastic simulations of neuronal vesicle release models. *Physical Biology* 7, 2 (may 2010), 026008. https://doi.org/10.1088/1478-3975/7/2/026008

[22] S. Nadkarni and P. Jung. 2007. Modeling synaptic transmission of the tripartite synapse. *Phys. Biol.* 4, 1 (2007).

[23] S. Nadkarni, P. Jung, and H. Levine. 2008. Astrocytes optimize the synaptic transmission of information. *PLoS Comput Biol* 4, 5 (May 2008), e1000088.

[24] A. Neishabouri and A. A. Faisal. 2014. Axonal noise as a source of synaptic variability. *PLoS Comput Biol* 10, 5 (May 2014), e1003615.

[25] J. T. Porter and K. D. McCarthy. 1996. Hippocampal astrocytes in situ respond to glutamate released from synaptic terminals. *J Neurosci* 16, 16 (Aug 1996), 5073–5081.

[26] H. Ramezani and O. B. Akan. 2017. A Communication Theoretical Modeling of Axonal Propagation in Hippocampal Pyramidal Neurons. *IEEE Trans. Nanob.* 16, 4 (2017).

[27] H. Ramezani and O. B. Akan. 2017. Importance of vesicle release stochasticity in neuro-spike communication. In *2017 39th Annual International Conference of the IEEE Engineering in Medicine and Biology Society (EMBC).*

[28] A. Ahmadzadeh S. Lotter and R. Schober. 2021. Synaptic channel modeling for DMC: Neurotransmitter uptake and spillover in the tripartite synapse. *IEEE Trans. Commun.* 69, 3 (2021).

[29] J. W. Shuai and P. Jung. 2002. Stochastic properties of Ca^{2+} release of inositol 1,4,5-trisphosphate receptor clusters . *Biophys. J.* 83, 1 (2002).

[30] S. G. Tewari and K. K. Majumdar. 2012. A mathematical model of the tripartite synapse: astrocyte-induced synaptic plasticity. *J Biol Phys* 38, 3 (Jun 2012), 465–496.

[31] M. Veletić, F. P. Anders, Y. Chahibi, and I. Balasingham. 2016. On the Upper Bound of the Information Capacity in Neuronal Synapses. *IEEE Transactions on Communications* 64, 12 (2016), 5025–5036. https://doi.org/10.1109/TCOMM.2016.2613970